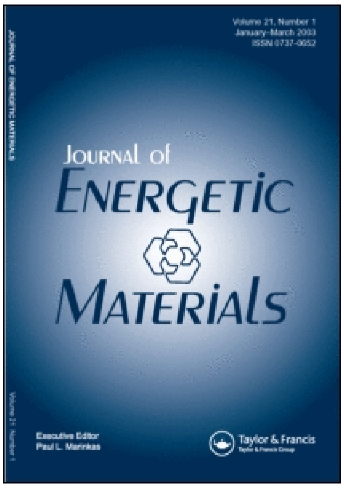

Journal of Energetic Materials
Publication details, including instructions for authors and subscription information:
http://www.informaworld.com/smpp/title~content=t713770432

Formation of Aluminum Nanoparticles upon Condensation from Vapor Phase for Energetic Applications

R. Schefflan[a]; S. Kovenklioglu[a]; D. Kalyon[a]; M. Mezger[b]; M. Leng[b]
[a] Stevens Institute of Technology, Highly Filled Materials Institute, Hoboken, NJ [b] U.S. Army, Armament Research Dev. & Eng. Center, NJ

To cite this Article Schefflan, R. , Kovenklioglu, S. , Kalyon, D. , Mezger, M. and Leng, M.(2006) 'Formation of Aluminum Nanoparticles upon Condensation from Vapor Phase for Energetic Applications', Journal of Energetic Materials, 24: 2, 141 — 156

To link to this Article: DOI: 10.1080/07370650600672041

URL: http://dx.doi.org/10.1080/07370650600672041

Journal of Energetic Materials, 24: 141–156, 2006

ISSN: 0737-0652 print/1545-8822 online
DOI: 10.1080/07370650600672041

Formation of Aluminum Nanoparticles upon Condensation from Vapor Phase for Energetic Applications

R. SCHEFFLAN
S. KOVENKLIOGLU
D. KALYON

Stevens Institute of Technology, Highly Filled
Materials Institute, Castle Point on Hudson,
Hoboken, NJ

M. MEZGER
M. LENG

U.S. Army, Armament Research Dev. & Eng. Center,
Picatinny Arsenal, NJ

A mathematical model of the nanoparticles formation process from deposition from the vapor phase process was developed and applied to the manufacture of alumina-coated aluminum nanoparticles. This process involves conversion of gaseous aluminum in the presence of helium carrier gas to solid aluminum nanoparticles. These activities effectively prepare the aluminum for reaction with oxygen gas to create an alumina coating in the remainder of the process.

The basis of the calculations is the General Dynamic Equation for aerosols, which was formulated as an explicit numerical equation. The equation is solved over a user specified surface with particle volume (equivalent to

Address correspondence to R. Schefflan, Stevens Institute of Technology, Highly Filled Materials Institute, Castle Point on Hudson, Hoboken, NJ 07030. E-mail: rscheffl@stevens.edu

particle diameter) and reactor holding time as the independent variables. The solution produces the number distribution function of the nanoparticles over the solution space. After all of the gaseous aluminum has solidified, a moment equation is employed to calculate the number of particles in each of the size distribution ranges.

The mathematical model is useful to study the trends on the dependence of the nanoparticle size distribution on the operating parameters such as pressure and temperature profile in the reactor. A number of case studies are included to demonstrate the utility of the mathematical model.

Keywords: aluminum nanoparticles, General Dynamic Equation, vapor phase process

Introduction

Nanocrystalline metals for which the grain size is the nanometer range (typically 10 to 100 nm) exhibit physical properties, which are significantly different than those of bulk polycrystalline materials and thus are used in multiple applications. For example, mixtures of oxidizers and fuels with particle sizes in the nanometer range form metastable intermolecular composites (subclass of thermites) to achieve higher densities, and higher combustion velocities [1].

One of the methods for the manufacture of nanoparticles involves condensation from the vapor phase. The process utilizes an inert carrier gas, at appropriate pressure. Metal is introduced onto a crucible and is molten. The metal is quickly taken to temperatures far above the melting point, but less than the boiling point, so that an adequate vapor pressure is achieved [2]. The carrier gas is continuously introduced into the chamber to move the evaporated metal away from the hot element. As the gas cools the metal vapor, nano-sized particles form. At this point the nanoparticles are very reactive, so they are coated with a material that prevents further interaction with other particles (agglomeration) or with other materials [2]. The typical process is shown in Fig. 1. The motivation to develop a mathematical model was based on the difficulty in developing an empirical scale-up of the process.

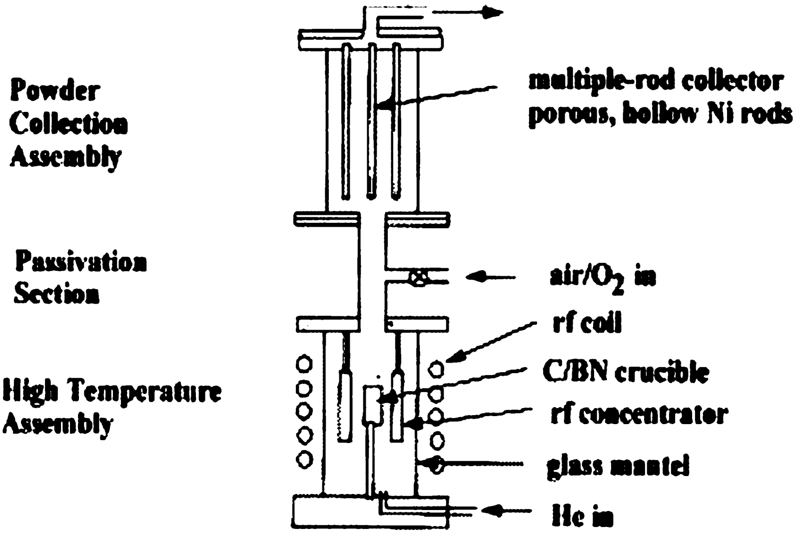

Figure 1. System which is mathematically modeled.

The lab-scale process is carried out in a clear tubular reactor in which a plug of aluminum, located at the entry to the reactor, is heated with microwave energy such that aluminum gas is produced. The gas is continuously mixed with a helium feed. Somewhere in the middle of the reactor, a second feed of oxygen gas is introduced. At this point all of the alumina has solidified into nanoparticles. The oxygen reacts with the surface aluminum to form alumina. This passivates the nanoparticles.

Scanning electron microscopy and transmission electron microscopy (TEM) techniques were used to investigate the size distributions and the surface characteristics of Al nanopowders. Transmission of electrons through the conductive sample and the use of proper X-ray detector with TEM allowed obtaining clear images with relatively high resolutions. In transmission electron microscopy very small amounts of sample were placed on a carbon-coated copper surface and the measurements were carried out. SEM microscopy studies were carried out with a Leo 982 Digital Field

Emission SEM with Schottky field-emission source, upper secondary electron detector, low voltage (500–1500 eV), high-resolution (1 nm) imaging conducting specimens, and Oxford UTW X-ray detector.

The typical nanoparticles which form and the passivation of the surface upon the formation of the oxide layer are shown in Figs. 2–4. Aluminum particles with relatively narrow size distribution are seen in Fig. 2 (SEM). Higher magnification with 20 nm scale in Fig. 3 (using TEM) reveals that the particles have spherical shapes with a typical size of 20–40 nm. It is also noticed that there are few particles with a size range of 40–58 nm. Another interesting feature is the oxide layer formation around the particles as seen in Fig. 4. The oxide layer is clearly seen and exhibits a thickness of 2.8 nm for a 48 nm particle.

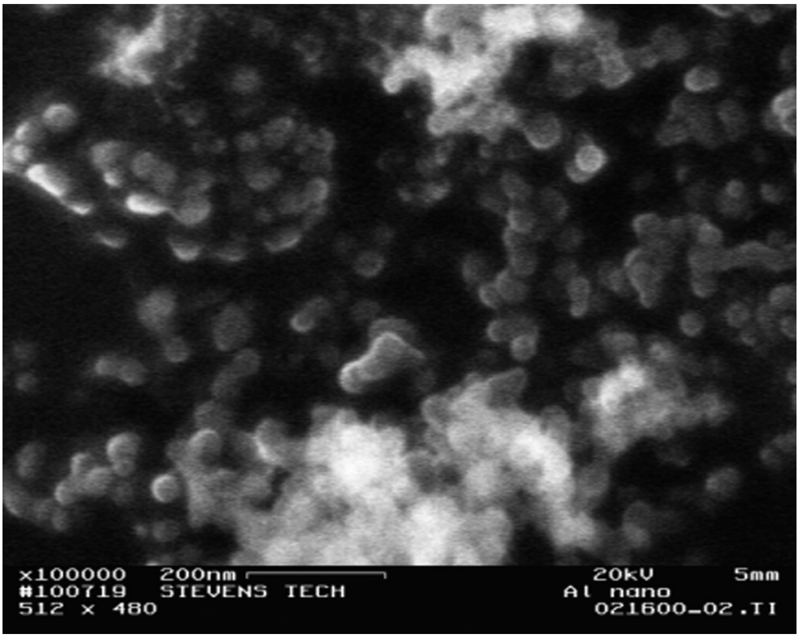

Figure 2. Typical SEM micrographs of nanoparticles.

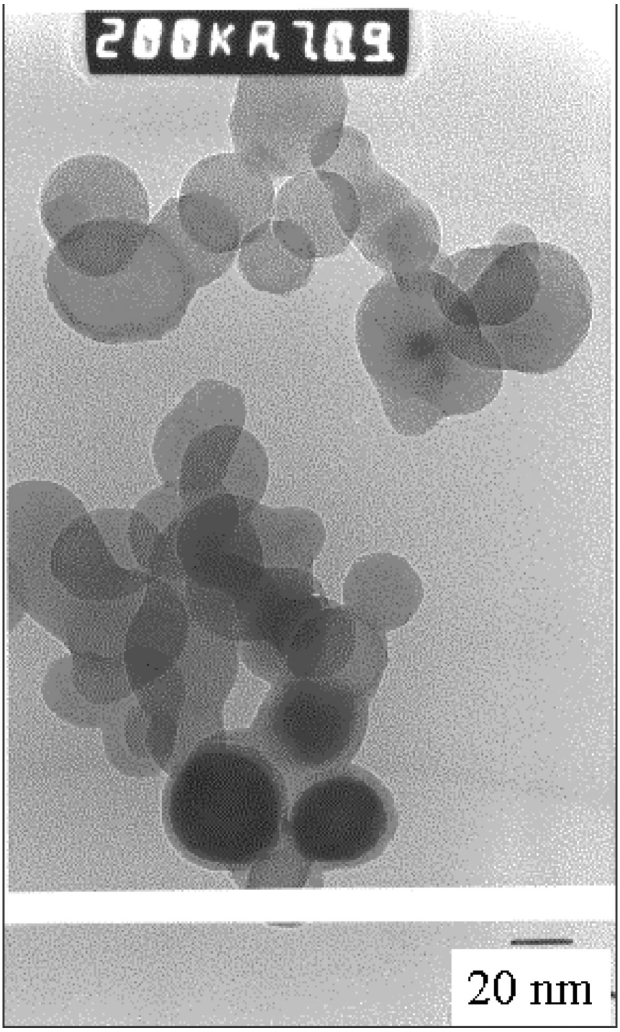

Figure 3. Typical shape and sizes of nanoparticles.

Methodology

The basis of the calculations is the General Dynamic Equation (GDE)(3), which is a complete description of the aerosol dynamics in terms of a particle size distribution function and

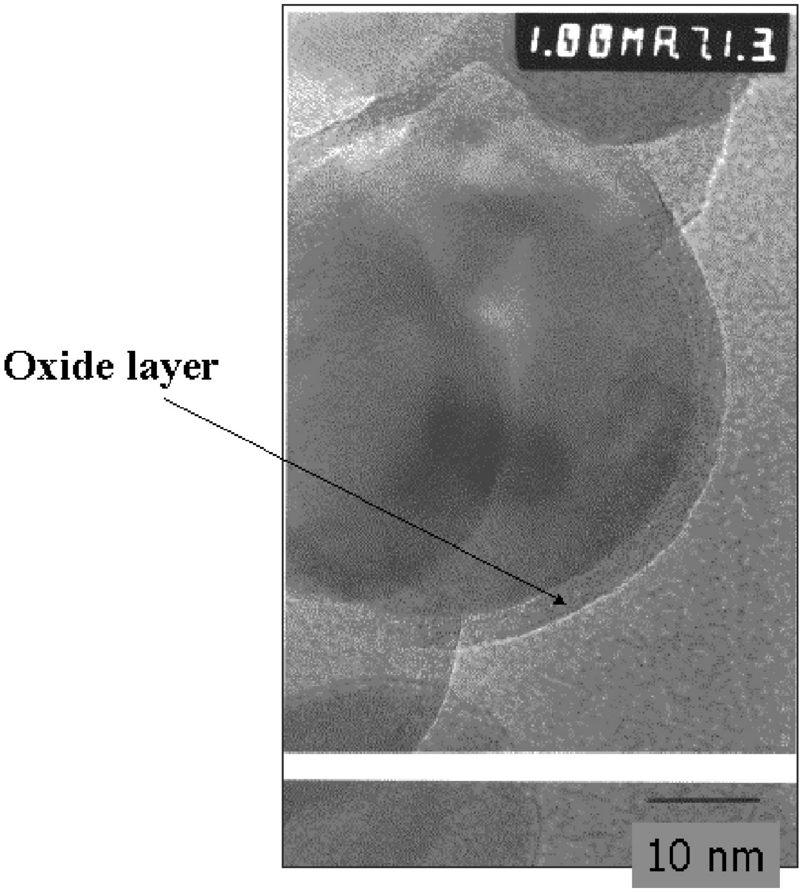

Figure 4. Nanoparticles with oxide layer visible.

is given by Equation (1) below:

$$\begin{aligned}\frac{\partial n}{\partial t}+\frac{\partial Gn}{\partial t}-I(v^*)\delta(v-v^*)=&\frac{1}{2}\int_0^v \beta(v-V,V)n(v-V,t)\\ &\times n(V,t)dV-n(v,t)\\ &\times\int_0^\infty \beta(v,V)n(V,t)dV\end{aligned}\tag{1}$$

where n is the particles size distribution function, G is the growth law, v is the particle volume, I(v*) is the nucleation rate, the delta function following the I(v*) is a Dirac function and β is the collision frequency. Particle growth is by Brownian coagulation and is represented by the two integrals. The first integral accounts for formation of particles of size v by coagulation of smaller particles. The second integral accounts for the loss of particles of size v by coagulation with all other particles. The theory of Brownian Coagulation [4] employs the collision frequency function given by Equation (2) below:

$$\beta(\mathrm{v}_i, \mathrm{v}_j) = 2k_b \frac{T}{3\mu}\left[\frac{1}{\mathrm{v}_i^{1/3}} + \frac{1}{\mathrm{v}_j^{1/3}}\right] \tag{2}$$

where k_b is Boltzmann's constant, T is the temperature, and μ is the viscosity.

Since the contact time has been observed to be extremely short we assume that growth is negligible.

The nucleation rate is determined from classical nucleation theory [3,5], which describes the homogeneous nucleation of dilute mixture of solids or liquids from a gas. The theory suggests that clusters of monomers are held together by van der Waals forces. The nucleation rate is given by Equation (3) below:

$$I = \left[\frac{p_1}{(2\pi m_1 k_B T)^{1/2}}\right]\left[\frac{2v_1\sigma^{1/2}}{(k_B T)^{1/2}}\right] n_1 \exp\left[\frac{-16\pi v_1^2\sigma^3}{3(k_B T)^3(\ln S)^2}\right] \tag{3}$$

Here p_1 is the partial pressure of aluminum, v_1 is the molecular volume, σ is surface tension, and S is the partial pressure of aluminum in the gas divided by its' vapor pressure.

The clusters become stable at a critical size d_p^*, equivalent to the critical volume, ν given by the Kelvin Equation shown below:

$$d_p^* = \frac{4\sigma v_1}{k_b T \ln S} \tag{4}$$

Model Development

The solution to the GDE was developed as an explicit discretization of the partial differential equation. The solution space for the GDE is divided into a grid incremented in particle volume v, and contact time t. The contact time is calculated by discretizing the total reactor volume and dividing an element of reactor volume by the flow rate of gas entering that element. Thus the solution develops by a repeated solution of a numerical version of the GDE at each element of reactor volume for all increments of particle size. The integrals on the right hand side of the equation are repeatedly solved, numerically, for use in the solution of the GDE. The explicit formulation was developed using a forward difference for the first term in the equation. The Nucleation Equation together with the Kelvin Equation are used to calculate the nucleation rate at each time step and the integrals calculated numerically at each step in particle volume. The complete formulation is given in numerical form as Equation (5) below:

$$n_{v,t+\Delta t} = n_{v,t} + \Delta t\left[I(\mathrm{v}^*)\delta(\mathrm{v} - \mathrm{v}^*) + \frac{1}{2}\mathrm{INT}_1 - n_{v,t}\mathrm{INT}_2\right] \quad (5)$$

where INT_1 and INT_2 represent the first and second integrals in the GDE.

The technique employed is to establish the grid size after which the numerical GDE is solved at each discrete value of v, particle size, at a specific t, time (which corresponds to an increment in reactor volume). After all $\mathrm{n}_{\mathrm{v,t}}$ are calculated, a material balance is performed to check that all of the aluminum has not been converted to particles at that particular time. The reactor volume is then incremented, the next time value calculated by reactor volume increment divided by entering gas flow rate and the entire process is repeated until no more aluminum is left in the vapor phase. When the GDE calculations end the last set of distribution function values are repeatedly integrated with respect to volume size, between each set of values ranging over 10 percent of the volume size, for example between 40 and 50 percent of the full range of particle sizes. This is the first moment of the distribution function with respect to v and gives the number of particles in that size range and is shown below:

$$N = \int_a^b n(v,t)dv \tag{6}$$

Here, n(v,t) represents the values of the distribution function at time t, varying between sizes a and b.

Model Implementation

The numerical version of the GDE in conjunction with the various required analytical equations was implemented. The program offers two possibilities

1. Exploration of the process conditions to determine the desired initial particle size and the nucleation rate.
2. Calculation of the distribution function.

Nucleation and Distribution Function Calculations

The input required to make a nucleation run involves the specification of various parameters including the gas flow rate and pressure and the geometry of the reactor along with the vapor pressure, the surface tension, melting temperature of the metal, the molecular weight, density, gas viscosity, evaporation rate of the metal, and the nucleation rate. This type of run must be made prior to attempting an aerosol-modeling run. When a modeling run is made the program converts the nucleation rate to its' equivalent value in distribution function units i.e., division by d_p^*. The input for the distribution function calculations requires the definition of the temperature profile along the reactor volume.

Figure 5 gives a plot of the distribution function at various reactor contact times. Figure 6 shows the number of particles in 10 percent size range increments at the end of the run, and Figure 7 shows the driving force for particle formation at various reactor contact times, i.e., the partial pressure of metal in the gas relative to its vapor pressure.

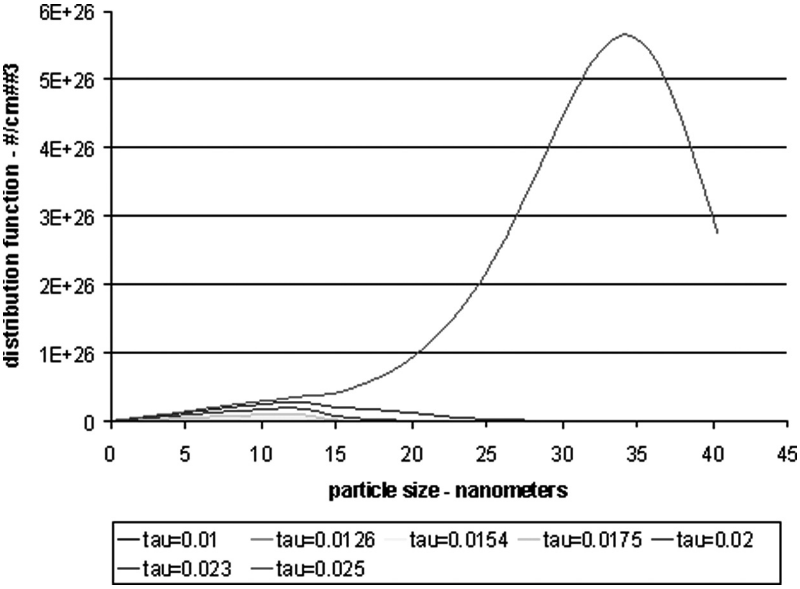

Figure 5. Particle distribution function at various contact times.

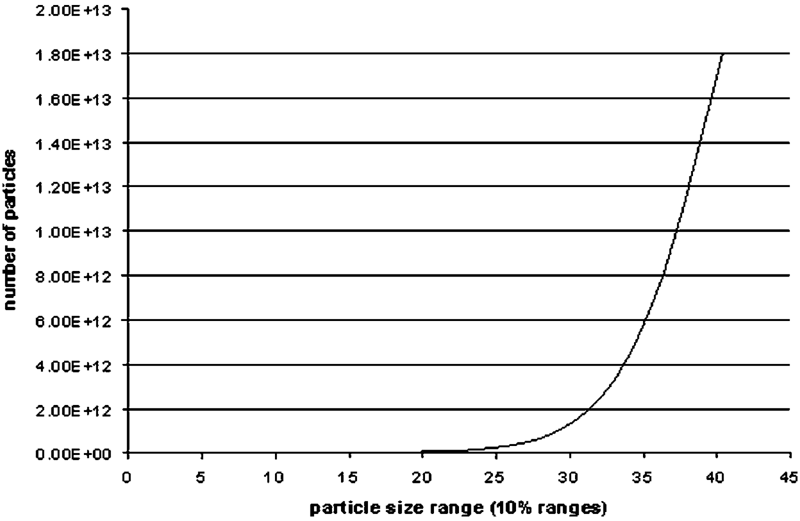

Figure 6. Typical growth of number of particles in ten percentile ranges.

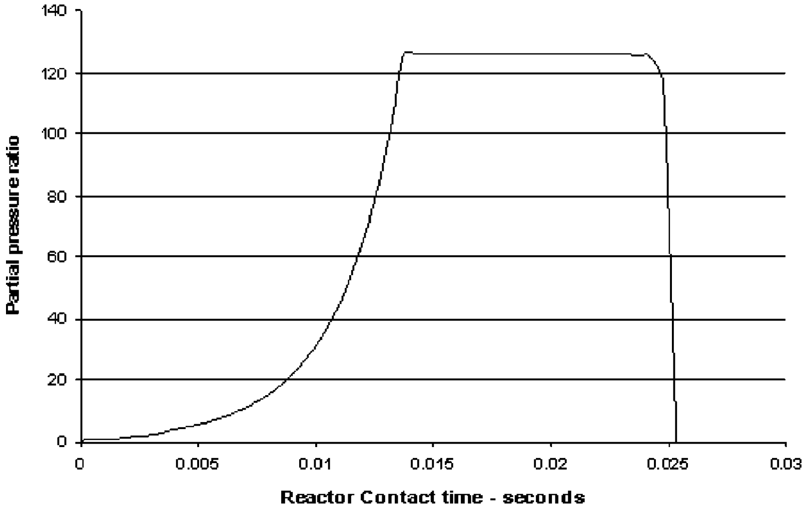

Figure 7. Driving force for particle formation.

Solution Method

The solution technique employed in the program is an explicit equation similar to an Euler solution to a differential equation. Though this method provides no internal error control, the approximations to the derivatives improve as the step size decreases. Complicating factors that are difficult to assess involve the fact that two numerical integrations are performed at each step in particle size, and one integration is performed at each reactor volume step. It is important that users develop solutions that are specific to their problem, at various step sizes to assure that they achieve a solution without excessive error. An example of the development of such a solution is given in Fig. 8 in which the solution grid varied between 100×50 to 200×100. Here, the distribution function at the reactor volume step immediately prior to the disappearance of gaseous aluminum is plotted. Only the larger grids used are shown in the figure. It appears that the solutions are about the same and therefore acceptable.

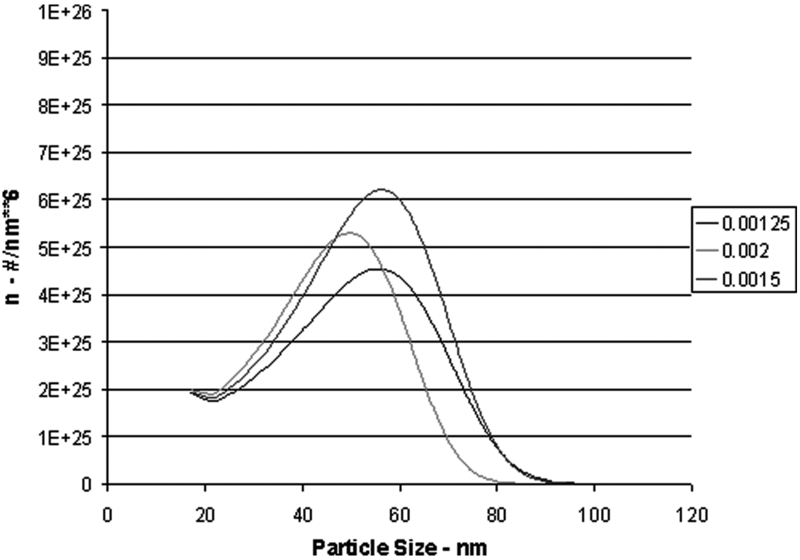

Figure 8. Solutions at different grid sizes.

Examples of Case Studies

Boiling or Temperature Controlled Liquid Metal Pool

Figure 9 shows two comparable solutions, one in which the material rapidly cools to the same temperature at which the second curve is controlled at. Initially the temperature of the boiling material is too high to form nuclei whereas in the temperature controlled calculation nuclei form immediately. This results in a delay of aerosol formation (57 reactor volume steps) in the boiling calculation relative to the one that is temperature controlled. There are also differences in the distribution function in that a greater number of particles of mean size are formed in the boiling case. Another difference is that the number of volume steps (of equal size) during which the aerosol is formed, required to bring the vapor to its saturated condition is considerably less (25 reactor volume steps) in the isothermal case than in the boiling case. The importance of these factors can only be evaluated in light of the process design, but the model can be used to focus attention on them.

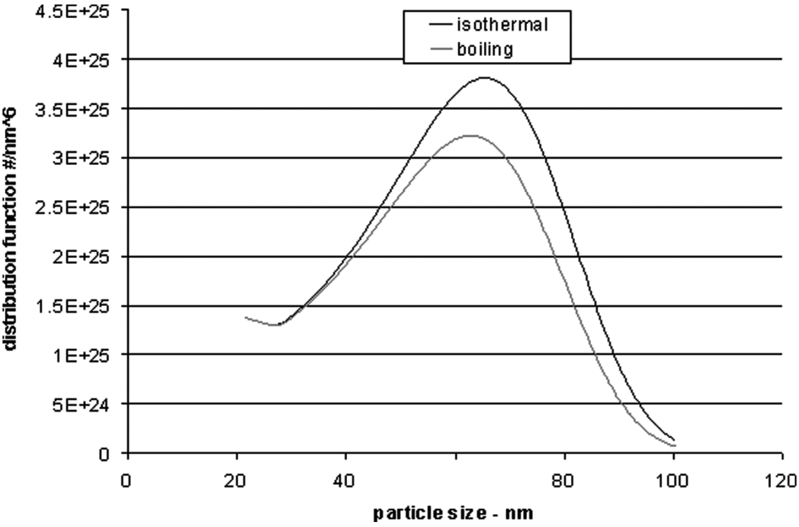

Figure 9. Solutions for the nanoparticle size distributions obtained upon differing reactor conditions.

Effect of Pressure with Constant Temperature Distribution along Length of Reactor

System pressure has a pronounced effect on nucleation rate and critical particle size, see Table 1. A reduction in pressure produces a lower saturation ratio accompanied by a reduction in the nucleation rate. Figure 10 shows these effects on the system,

Table 1
Effect of pressure

Pressure mm Hg	Temperature deg. C	Saturation ratio	Mole fraction vapor	Nucleation rate number/ cm**3/sec
10	1025	134.01097	0.196601334	3.98805E + 15
6	1025	118.48185	0.289698779	1.05672E + 15
5	1025	111.993	0.328599557	5.5953E + 14
4	1025	103.49121	0.379567979	2.22187E + 14

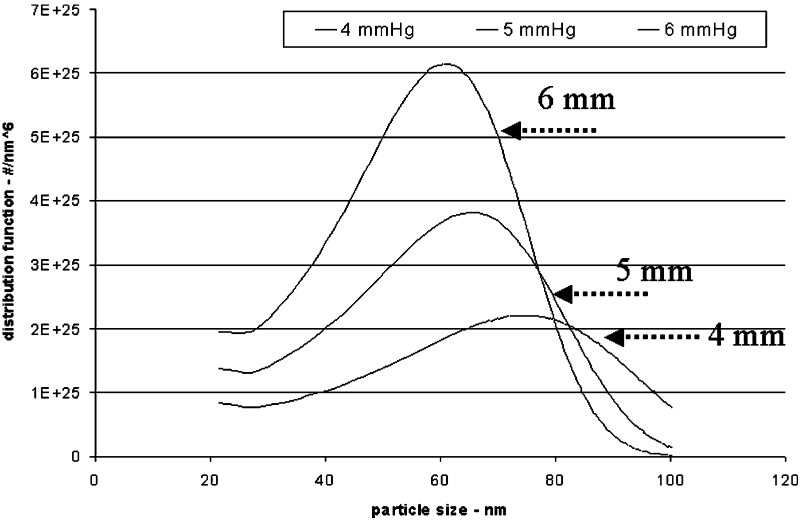

Figure 10. Solutions for the nanoparticle size distributions obtained upon differing pressure conditions in the reactor.

with the lower pressure yielding a relatively wider range of particle sizes being produced with a larger mean particle size but fewer particles.

Effect of Temperature Distribution along Length of Reactor at Constant Pressure

Two constant pressure runs were made with the model while imposing two different temperature profiles on the system. Both employed an initial temperature of 1025 degrees Centigrade. The first run had a linear temperature profile imposed ending at about 700 degrees Centigrade near the reactor position at which all of the aluminum in the vapor phase had condensed. The second run employed a constant temperature of 1025 degrees Centigrade. The results are shown in Figs. 11 and 12.

The results are pronounced as one may observe that the isothermal case yields a relatively wide particle size distribution ranging from about 30 to 100 nanometers with a mean of about

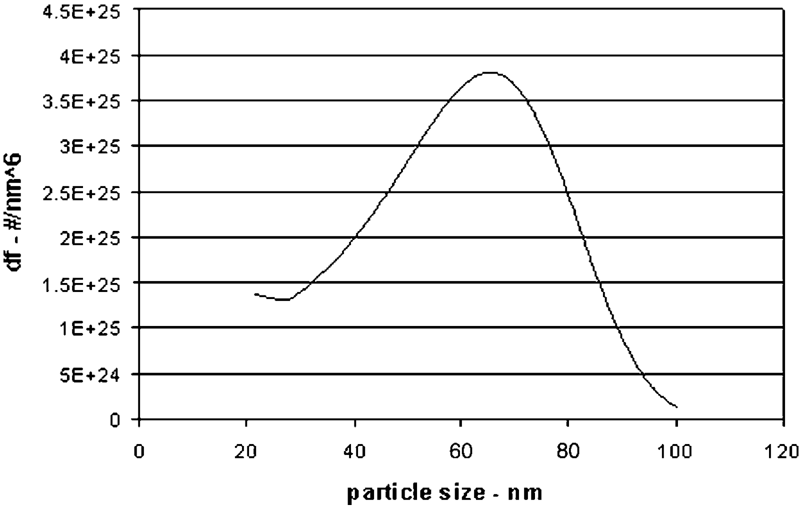

Figure 11. Solution for the nanoparticle size distribution obtained using a linear temperature profile in the reactor (ending at 700°C).

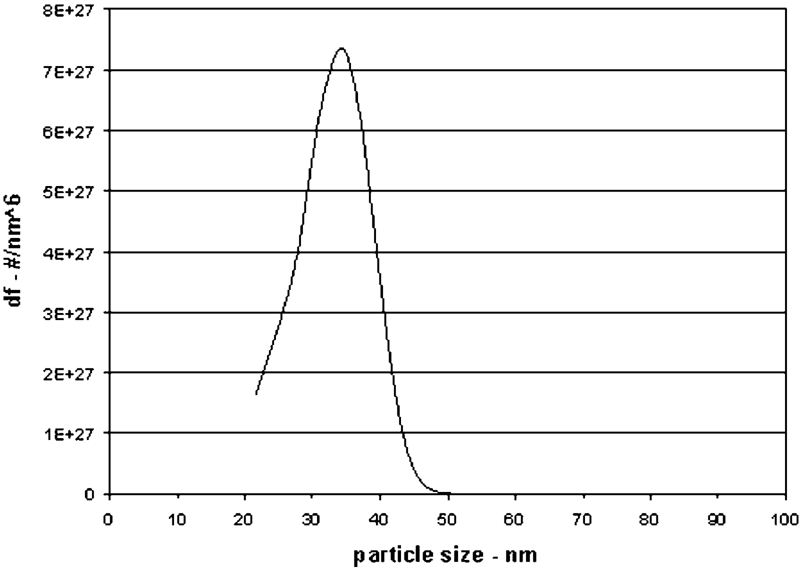

Figure 12. Solution for the nanoparticle size distribution obtained using isothermal reactor (at 1025°C).

65 nanometers and distribution function values on the order of 10^{27}, whereas the imposed linear temperature profile produces a particle size distribution ranging from about 20 to 50 nanometers with a mean of about 35 nanometers and with distribution function values on the order of 10^{25}. Variations on these possibilities may be a means by which particle size distribution is controlled.

Acknowledgements

We are grateful for the funding of the US Army ARDEC under contract DAAE30-97-D-1009 T12, which made this study possible. We thank Messers. T. McWilliams, A. Perich and D. Fair of ARDEC for their support and Prof. M. Libera of Stevens for the TEM analysis of the nanoalumina. This paper was presented at the *199th Meeting of the Electrochemical Society on March 27, 2001 in the "Fundamental Gas-Phase and Surface Chemistry of Vapor Deposition II and Process Control, Diagnostics and Modeling Symposium", Washington, DC with the abstract of the paper appearing in the Proceedings of the Symposium.*

References

[1] Perry, W. L., B. Smith, C. Bulian, J. Busse, C. Macomber, R. Dye, and S. Son. 2004. Nano-scale tungsten oxides for metastable intermolecular composites. *Propellants, Explosives and Pyrotechnics*, 29(2): 99–105.

[2] http://www.azonano.com

[3] Friedlander, S. K. 1977. *Smoke, Dust and Haze*. New York: Wiley Interscience.

[4] Hidy, G. M. and J. R. Brock. 1970. *The Dynamics of Aerocolloidal Systems*, Oxford: Pergamon Press.

[5] Seinfeld, J. H. 1986. *Atmospheric Chemistry and Physics of Air Pollution*. New York: Wiley Interscience.